Molecular Pharmacology Fast Forward. Published on June 14, 2016 as DOI: 10.1124/mol.115.102988
This article has not been copyedited and formatted. The final version may differ from this version.

HSP90 regulation of P2X7 receptor function requires an intact cytoplasmic C-terminus

Keisuke Migita, Taku Ozaki, Shuji Shimoyama, Junko Yamada, Yoshikazu Nikaido, Tomonori Furukawa, Yuko Shiba, Terrance M. Egan, and Shinya Ueno

Department of Drug Informatics, Faculty of Pharmaceutical Sciences, Fukuoka University, Fukuoka, Japan (K.M); Department of Neurophysiology (T.O., S.S., Y.N., T.F., Y.S., S.U.) and Research Center for Child Mental Development (T.O., S.S., S.U.), Hirosaki University Graduate School of Medicine, Hirosaki, Aomori, Japan; Department of Biomedical Sciences, Hirosaki University Graduate School of Health Sciences, Hirosaki, Aomori, Japan (J.Y.); and Department of Pharmacology and Physiology, and The Center for Neuroscience, Saint Louis University School of Medicine, St. Louis, Missouri, USA (T.M.E.)

Molecular Pharmacology Fast Forward. Published on June 14, 2016 as DOI: 10.1124/mol.115.102988
This article has not been copyedited and formatted. The final version may differ from this version.

Running title: HSP90 modulates P2X7 receptor function via C-terminus

To whom correspondence should be addressed:

Keisuke Migita

Department of Drug Informatics, Faculty of Pharmaceutical Sciences, Fukuoka University,

8-19-1 Nanakuma, Jounan-ku, Fukuoka 814-0180, Japan

Tel.: +81-92-871-6631

Fax: +81-92-863-0389

E-mail: migitak@fukuoka-u.ac.jp

The number of text pages: 35

The number of tables: 4

The number of figures: 9

The number of references: 43

The number of words in the Abstract: 146

The number of words in the Introduction: 535

The number of words in the Discussion: 1255

ABBREVIATIONS: HSP90, heat shock protein 90; $NMDG^+$, N-methyl-D-glucamine$^+$; ATP, adenosine triphosphate; TM, transmembrane domain; EC_{50}, half maximal effective concentration; Bz-ATP, 2'(3')-*O*-(4-Benzoylbenzoyl)adenosine-5'-triphosphate; 17-AAG, 17-*N*-allylamino-17-demethoxygeldanamycin; 17-DMAG, 17-Dimethylaminoethylamino-17-demethoxygeldanamycin

Molecular Pharmacology Fast Forward. Published on June 14, 2016 as DOI: 10.1124/mol.115.102988
This article has not been copyedited and formatted. The final version may differ from this version.

Abstract

P2X7 receptors (P2X7Rs) are ATP-gated ion channels that display the unusual property of current facilitation during long applications of agonists. Here we show that facilitation disappears in chimeric P2X7Rs containing the C-terminus of the P2X2 receptor (P2X2R), and in a truncated P2X7R missing the cysteine-rich domain of the C-terminus. The chimeric and truncated receptors also show an apparent decreased permeability to $NMDG^+$. The effects of genetically modifying the C-terminus on $NMDG^+$ permeability were mimicked by pre-application of the HSP90 antagonist geldanamycin to the wild-type receptor. Further, the geldanamycin decreased the shift in the reversal potential of the ATP gated current measured under bi-ionic $NMDG^+/Na^+$ condition without effecting the ability of the long application of agonist to facilitate current amplitude. Taken together, the results suggest that HSP90 may be essential for stabilization and function of P2X7Rs through an action on the cysteine-rich domain of the cytoplasmic C-terminus.

Molecular Pharmacology Fast Forward. Published on June 14, 2016 as DOI: 10.1124/mol.115.102988
This article has not been copyedited and formatted. The final version may differ from this version.

Introduction

P2X receptors (P2XRs) are a family of seven ATP-gated ion channels that underlie a diverse array of functions in both simple and complex organisms (North, 2002). All seven members of the family (P2X1R – P2X7R) are composed of three subunits, and show a preference for cations over anions (Nicke et al, 1998; Barrera et al, 2005; Egan et al, 2006). Each subunit has intracellular N- and C-termini and two transmembrane domains (TM1 and TM2) separated by a large extracellular loop (Surprenant et al, 1996; Egan et al, 2004). By comparison to all other family members, the C-terminus of P2X7R is longer and contains a unique cysteine rich domain (Erb et al, 2006; Egan et al, 2006; Costa-Junior et al, 2011). Channels with truncated C-termini missing this domain show an apparent decreased ability to transport large (up to 900 Da) polyatomic molecules during long applications of ATP (Surprenant et al, 1996; Khakh et al, 1999), suggesting that this cytoplasmic domain plays a role in regulation of current through the channel. Recently, high resolution structures of the zebrafish P2X4.1 receptor (zfP2X4.1R) were obtained in the presence and absence of ATP, leading to a much better understanding of the conformational changes underlying channel gating (Kawate et al, 2009; Hattori and Gouaux, 2012). However, these structures lack the cytoplasmic N- and C-termini, and the manner in which the cytoplasmic domains regulate channel function therefore is still open to question. One possibility suggested by proteomic studies is that the C-terminus contains a binding site for regulatory proteins such as laminin α3, integrin kinase, and the heat shock proteins HSP70, HSP71 and HSP90 that are capable of altering channel properties (Kim et al, 2001; Gu et al, 2009). The presence of an HSP90 is particularly intriguing because this heat shock protein is thought to repress P2X7R function (Adinolfi et al, 2003) and play a role in caspase-dependent

Molecular Pharmacology Fast Forward. Published on June 14, 2016 as DOI: 10.1124/mol.115.102988
This article has not been copyedited and formatted. The final version may differ from this version.

apoptosis of rodent macrophages and microglia (Levin et al, 2008; Chen et al, 2009).

In the present report, we sought to determine if HSP90 regulates ATP-gated current by interacting with the C-terminus of the P2X7R. Some (P2X2R, P2X4R, P2X7R) but not all P2XRs show an apparent time-dependent increase in permeability to large organic cations such as N-methyl-D-glucamine$^+$ ($NMDG^+$), ethidium$^+$, and the carbocyanine nucleic acid dye, YO-PRO-1 (Khakh et al, 1999; Virginio et al, 1999; Yan et al, 2008; Yan et al, 2010). In the case of the P2X7R, the time-course of the apparent change in cation permeability is associated with an increase in charge transfer across the membrane (called "current facilitation") (Yan et al, 2008; Yan et al, 2010; Khadra et al, 2013; Rokic et al, 2013). In contrast, the long applications of ATP needed to induce the permeability changes of P2X2Rs results in a decrease in charge transfer because the receptor desensitizes (Khakh et al, 1999; Coddou et al, 2015). The different time-dependent effects of ATP on the size of P2X2R and P2X7R currents suggest that chimeras of these channels may be useful tools to determine the locus of the HSP90 effect on P2X7R function. Here, we report findings suggesting that HSP90 plays an important role for stabilization and function of P2X7R by interacting with the cysteine-rich domain of the C-terminus of the P2X7R.

Molecular Pharmacology Fast Forward. Published on June 14, 2016 as DOI: 10.1124/mol.115.102988
This article has not been copyedited and formatted. The final version may differ from this version.

Materials and Methods

Cell culture and heterologous expression of recombinant receptors. HEK293 or HEK293T cells were maintained in Dulbecco's modified Eagle medium (Sigma-Aldrich, St. Louis, MO, USA) containing 10% fetal bovine serum and 100 U/ml penicillin-streptomycin (Gibco-Invitrogen, Carlesbad, CA, USA). These cells were plated at a density of 100,000 cells per 35 mm culture dish and kept at 37 °C in a humidified atmosphere containing 5% CO_2. Cells were co-transfected with 1.0 μg of cDNA encoding a rat wild-type or mutant P2X7R, and 0.5 μg of a DsRed expression plasmid using 4 μl of Attractene according to the manufacturer's protocols (Qiagen, Sussex, UK). Large ATP-gated currents through functional receptors were studied 24-36 hrs post- transfection.

Generation of chimeric P2X7Rs. Chimeras were constructed by performing two successive PCR amplifications using 5' and 3' primers containing overlapping regions between rat P2X2Rs and P2X7Rs in pcDNA3.1(+). To generate a chimera consisting of the P2X7R with the N-terminal domain of P2X2R, we used overlap oligonucleotides encoding the sequences RNRRL/GTIKWIL (corresponding to aa 25–29 for P2X2R and aa 27–33 for P2X7R). To generate a chimera consisting of P2X7R with the C-terminal domain of P2X2R, we used overlap oligonucleotides encoding aa LIINT/FMNKNKL (corresponding to aa 353–357 for P2X7R, aa 355–361 for P2X2R). Each 25 μl PCR reaction contained 0.1 μg of the template P2XR, 500 pmol of each primer, 125 μM dNTPs, and 2.5 units/ml PFU or GXL DNA polymerase (Takara DIO INC., Shiga, Japan). PCR parameters included an initial denaturation at 95 °C for 1min followed by 30 cycles (95°C for 10 sec, 55 ~ 60°C for 5 sec, 68°C for 60 sec and 3 min). The first PCR product was purified by mini-prep (Qiagen, Sussex, UK), and 1 μl of the product was

Molecular Pharmacology Fast Forward. Published on June 14, 2016 as DOI: 10.1124/mol.115.102988
This article has not been copyedited and formatted. The final version may differ from this version.

used as template DNA for the second PCR. All sequences were confirmed by DNA sequencing (FASMAC Co. Ltd., Kanagawa, Japan).

Immunocytochemistry. Cells were plated onto glass slides, and then transfected with cDNAs encoding wild-type and chimeric receptors as described above. The plated cells were then washed three times with 0.1 M sodium phosphate buffer (PBS), followed by fixation with 4% paraformaldehyde in PBS for 20 min at room temperature. After washing three times with PBS, cells were incubated with blocking solution (0.1% Triton X-100 and 5% donkey serum in PBS) for 30 min. Cells were then incubated with anti-P2X7R (1:1000, Alomone Labs, Jerusalem, Israel) in the blocking solution for 2 hrs at room temperature. After washing three times with PBS, cells were incubated with Alexa Fluor 488-conjugated donkey anti-rabbit (1:400, Molecular Probe, Eugene, OR, USA) for 1 hr at room temperature. After washing three times with PBS and rinse in distilled water, coverslips were mounted on slides with an anti-fading reagent.

Whole cell current recording and application of drugs. Immediately preceding the start of an experiment (Migita et al, 2001), plated cells were mechanically dispersed using a fire-polished Pasteur pipette, and an aliquot of the dispersion was transferred to a recording chamber. Cells predicted to express P2XR protein were identified using fluorescence microscopy to detect the presence of Ds-Red. Whole-cell current was measured at room temperature with low resistance (1.5-3 MΩ), lightly fire-polished, borosilicate electrodes from single cells held at -60 mV using a broken-patch method. The data were recorded with a Multiclamp 700B (Molecular Devices, Sunnyvale, CA, USA), filtered at 1 kHz and digitized at 10 kHz using a Digidata 1322A (Molecular Devices, Sunnyvale, CA, USA). Data acquisition and analysis were

Molecular Pharmacology Fast Forward. Published on June 14, 2016 as DOI: 10.1124/mol.115.102988
This article has not been copyedited and formatted. The final version may differ from this version.

performed using pClamp9.2 software (Molecular Devices, Sunnyvale, CA, USA) and Igor Pro software (WaveMetrics, Inc, Lake Oswego, OR, USA). The pipette solution contained (in mM): 140 CsCl, 1 $MgCl_2$, 10 EGTA, 10 HEPES (pH 7.4 with CsOH). The extracellular solution contained: 154 NaCl, 1 $MgCl_2$, 1 $CaCl_2$, 10 glucose, and 10 HEPES (pH 7.4 with NaOH). Drugs were applied for 1 sec or 60 sec once every 2-5 min using triple-barreled glass and a Perfusion Fast-Step System SF-77 (Warner Instruments, Hamden, CT). For estimates of activation and deactivation rates, cells were lifted from the substrate to increase speed of the concentration changes. The time-course of the concentration change was measured by switching the solution from normal external solution to solution containing 150 mM K^+. The 10-90% time for change in holding current was 9.8 ± 0.2 msec (switch into high K^+ solution; n = 19) and 5.9 ± 0.4 msec (switch back to normal bath solution; n = 19). Successive applications of ATP were separated by at least 3 min.

The current-voltage curve, obtained by ramping the voltage from -80 to 40 mV with 200 msec on every other second for 60 sec, was used to estimate changes in reversal potential during the application of either 30 μM (when studying P2X2R) or 3 mM (when studying P2X7R) ATP. To measure permeability changes, the extracellular solution contained no Ca^{2+} or Mg^{2+}, and the 154 mM NaCl was replaced by 154 mM NMDG-Cl; $MgCl_2$ was also removed from the pipette solution. From these data, we calculated the relative permeability as $P_{NMDG}/P_{Cs} = \exp(V_{rev}F/RT)$ where V_{rev} is the bi-ionic reversal potential measured in extracellular NMDG-Cl and intracellular CsCl, F is Faraday's constant, R is the universal gas constant, and T is the absolute temperature.

To construct concentration-response curves, peak agonist-gated current was normalized to that measured during application of 10 mM ATP in each cell. Individual curves were then fit

Molecular Pharmacology Fast Forward. Published on June 14, 2016 as DOI: 10.1124/mol.115.102988
This article has not been copyedited and formatted. The final version may differ from this version.

with the Hill equation ($I = I_{max} / [1+(X_{half} / X)^{rate}]$) using the Levenberg-Marquardt algorithm implemented in IGOR Pro, where *I* is the peak amplitude of the agonist-gated current and *X* is the agonist concentration. The fit was used to estimate the maximum current (I_{max}), the concentration of agonist needed to evoke a half-maximal current (X_{half}, also called the EC_{50}), and the Hill coefficient (n_H, equal to the *rate*). The values of each of these parameters were appropriately pooled to determine differences amongst groups.

Western Blots. HEK293T cells expressing P2X7R and P2X7R[Δ18] were cultured in 10 cm plates and treated with geldanamycin (5 μM, 20 min). Cells were washed twice with PBS, scraped from the dish, and centrifuged at 1000 g for 1 min at room temperature. The pellets were homogenized with a lysis buffer composed of 20 mM Tris-HCl at pH 8.0, 10 mM KCl, 1 mM $MgCl_2$, 1 mM EDTA, 10% glycerol and a protease inhibitor cocktail (cOmplete Protease Inhibitor Cocktail tablets, Roche Applied Science). This was then incubated on ice for 20 min, followed by centrifugation at 1000 g for 5 min at 4 °C. The protein-rich supernatant was centrifuged again at 3,300 g for 5 min at 4 °C, followed by an addition centrifugation at 6,000 g for 15 min at 4 °C to remove mitochondria. Finally, the resulting supernatant was centrifuged at 20,000 g for 1 hr at 4 °C. The pellet was treated with a second lysis buffer (20 mM Tris-HCl at pH 8.0, 150 mM KCl, 1 mM $MgCl_2$, 1 mM EDTA, 1% SDS and protease inhibitor cocktail). Protein concentration in lysate was determined by micro BCA protein assay kit (Life technologies, California, USA). Protein samples (10 μg) were diluted into the sample buffer (100 mM Tris-HCl, pH 6.8, 4% SDS, 20% glycerol, 10% β-mercaptoethanol), then boiled for 5 min, separated by SDS-PAGE on 10% gels, and transferred onto a methanol-activated polyvinylidene difluoride membrane (Immobilon-P, PVDF, Millipore). After blocking with 5% nonfat

Molecular Pharmacology Fast Forward. Published on June 14, 2016 as DOI: 10.1124/mol.115.102988
This article has not been copyedited and formatted. The final version may differ from this version.

milk/Tris-buffered saline solution containing 0.1% Tween 20 (TBS-T) for 1 hr at room temperature, the membrane was incubated with primary antibodies (anti-P2X7R, Alomone Labs; 1:10,000, anti-HSP90, BD Transduction Laboratories; 1:5,000 and anti-β-actin, Sigma-Aldrich; 1:10,000) at 4 °C for overnight and washed three times with TBS-T. Horseradish peroxidase-conjugated anti-mouse IgG (1:5,000, Jackson ImmunoResearch Laboratories) or anti-rabbit IgG (1:5,000, Jackson ImmunoResearch Laboratories) was used as a secondary antibody. The signals were detected by using an ECL (Bio-Rad).

Statistics. Statistical analysis of data was performed using the Student's *t* test for comparisons between two groups, or analysis of variance followed by Turkey's test for multiple comparisons using the statistics routines of Igor Pro. Results are expressed as means and standard error of the mean (S.E.M.). The level of significance was set at $P < 0.05$.

Chemicals. Geldanamycin was obtained from SERVA Electrophoresis GmbH (Heidelberg, Germany). 17-AAG and 17-DMAG were obtained from TOCRIS Bioscience (Bristol, UK). Other chemicals were purchased from Sigma-Aldrich (St. Louis, MO, USA).

Molecular Pharmacology Fast Forward. Published on June 14, 2016 as DOI: 10.1124/mol.115.102988
This article has not been copyedited and formatted. The final version may differ from this version.

Results

HSP90 interacts with P2XRs. P2X2Rs, P2X4Rs and P2X7Rs, but not P2X3Rs show apparent time-dependent changes in polyatomic cation permeability when exposed to agonist for several seconds (Khakh et al, 1999; North, 2002; Yan et al, 2008; Yan et al, 2010). Interestingly, P2X2R currents desensitize whereas P2X4R and P2X7R currents facilitate during extended exposure to agonists. Lalo and coworkers (Lalo et al, 2012) showed that human P2X1R currents were blocked and human P2X2R currents were potentiated by pre-application of the HSP90 antagonist, geldanamycin. We investigated the effects of geldanamycin on rat P2XRs (Fig. 1A), and found that currents through both rat P2X4Rs (amplitude of the second ATP-gated current divided the amplitude of the first equaled 0.67 ± 0.07 in the absence of geldanamycin and 4.81 ± 1.29 in the presence of geldanamycin) and rat P2X7R (ratios in the absence and presence of geldanamycin equaled 0.72 ± 0.10 and 2.28 ± 0.73, respectively) were potentiated by geldanamycin, whereas currents through the P2X2R and P2X3R were not (Fig. 1B). The ability of geldanamycin to potentiate human P2X2Rs (Lalo et al, 2012) but not rat P2X2Rs (Fig. 1) demonstrates important yet previously unappreciated species-dependent actions of HSPs on P2X receptors, and suggest that unique sites may be involved in HSP90 regulation of individual P2XRs.

Functional P2X2/7 chimeras are targeted to the cell surface membrane. We wondered if this difference of HSP90 regulation of rat P2X2Rs (no effect) and P2X7Rs (potentiation) reflects the variations in sequences of the N- and/or C-terminus. To investigate this hypothesis, we made P2X2/7 chimeric receptors in which parts of the P2X7R were replaced with parts of the P2X2R (Fig. 2A). We transfected HEK293 cells with genes encoding the chimeras, and studied them

Molecular Pharmacology Fast Forward. Published on June 14, 2016 as DOI: 10.1124/mol.115.102988
This article has not been copyedited and formatted. The final version may differ from this version.

using immunohistochemistry and electrophysiology. All of the chimeric proteins were expressed in transfected cells (Fig. 2B), and in all cases, the transfected cells showed measurable currents when challenged with ATP (Fig. 3). Current through the X7-X7-X2 chimera was smaller than that seen for the other constructs, but still large enough to allow accurate measurements of its properties (see below).

A role of the intracellular region of P2X7R in current facilitation. The wild-type P2X7R shows a biphasic response to long applications of ATP composed of an initial fast inward current called I_1 and a second, slower inward current called I_2 that grows larger in the continued presence of ATP (upper left panel of Fig. 3). All of the constructs showed similar densities of I_1 and I_2 currents with two exceptions (Table 1). First, the P2X7R chimera containing the C-terminus of the P2X2R (X7-X7-X2) showed a mono-phasic current that lacked an obvious I_2 component. Second, I_2 was significantly larger in the P2X7R containing the N-terminus of the P2X2R (X2-X7-X7). On the other hand, it tended to depend C-termini for 10-90% rise time and both N- and C-terminus or cysteine rich domain for decay time constant (Table 1). Although these results are interesting, the effects of domain swaps and mutations on the densities of I_1 and I_2 could reflect changes in protein assembly, protein trafficking, or channel kinetics. We did not further pursue these distinctions because the investigation of I_1 and I_2 *per se* is not the main goal of this study. More central to our project is the finding that the two mutant constructs with altered C-termini (X7-X7-X2 and X2-X7-X2) show significantly less facilitation than the wild-type receptor (see Table 1). Taken together, these results support the contention that facilitation of P2X7R current requires a full-length native C-terminal tail (Yan et al, 2008; Yan et al, 2010; Liang et al, 2015).

Molecular Pharmacology Fast Forward. Published on June 14, 2016 as DOI: 10.1124/mol.115.102988
This article has not been copyedited and formatted. The final version may differ from this version.

$NMDG^+$ permeability in P2X7 chimeric receptors. Next, we examined the effect of altering the structure of the P2X7R on the time-dependent change in the reversal potentials of the ATP-gated currents, measured when $NMDG^+$ or Cs^+ is the dominate carrier of cationic current, that coincides with the generation of I_2 during long applications of ATP (Fig. 4). We measured reversal potentials at the start (during I_1) and end (during I_2) of a 60 sec application of 3 mM ATP. For the wild-type P2X7R, the reversal potential shifted from -38.9 ± 1.7 to -13.0 ± 5.9 mV (n=6) as P_{NMDG}/P_{Cs} increased from 0.21 ± 0.01 to 0.67 ± 0.12. The shift in the reversal potential was smaller for the wild-type P2X2R (15.8 ± 5.3 mV, n=6), indicating that P_{NMDG}/P_{Cs} increased from 0.15 ± 0.01 to 0.28 ± 0.03. Most importantly, all of the chimeras showed much smaller changes in E_{rev} and P_{NMDG}/P_{Cs}, with the smallest changes occurring in the chimeric receptors containing the C-terminus of the P2X2R (Table 2). If indeed the shift in reversal potential reflects a change in NMDG+ permeability (see below), then these data support the contention that the C-terminus plays a significant role in $NMDG^+$ permeability of the P2X7Rs (Jiang et al, 2005; Yan et al, 2008; Yan et al, 2010).

Geldanamycin potentiates I_1 through an action on the C-terminus. The C-terminus of the P2X7R binds HSP90 in pull-down assays (Kim et al, 2001; Gu et al, 2009). Thus, we investigated the functional consequences of this interaction by determining the effect of the HSP90 antagonist, geldanamycin, on ATP-gated current (Fig. 5A). We found that the peak I_1 evoked by a 1 sec application of 3 mM ATP in the wild-type P2X7R increased 2.1 ± 0.5 fold after a 20 min application of geldanamycin (Fig. 5B, Table 3). Similar effects were seen using other HSP90 antagonists; peak I_1 evoked by a 1 sec application of 3 mM ATP in the wild-type P2X7R increased 2.0 ± 0.2 and 1.5 ± 0.1 fold after a 20 min application of 5 nM 17-AAG and

Molecular Pharmacology Fast Forward. Published on June 14, 2016 as DOI: 10.1124/mol.115.102988
This article has not been copyedited and formatted. The final version may differ from this version.

100 nM 17-DMAG, respectively (Supplemental Fig. 1). Further, geldanamycin tended to increase I_1 through the only chimeric receptor with an intact P2X7 C-terminus (X2-X7-X7) (see $I_1/I_{control}$ of Table 3). In contrast, the chimera with non-native (X7-X7-X2 and X2-X7-X2) C-termini failed to show increased ATP-evoked currents in the presence of geldanamycin.

We considered the following possible causes of the effect of geldanamycin on the initial phase of the P2X7R current. First, geldanamycin might alter the sensitivity of the P2X7R to ATP. This seems unlikely because we used super-maximal concentrations of ATP to evoke I_1 in these experiments (Fig. 5), and because the EC_{50}s measured in the presence and absence of geldanamycin were nearly identical (Table 4). Second, the increase in I_1 amplitude might result from an increase in protein expression of either the P2X7R channel or the putative accessory protein HSP90. However, we saw no changes in total or surface protein expression using Western blot analysis (Fig. 9A,B, Supplemental Fig. 2). The third possibility, that geldanamycin affects the ability of C-terminal domain of the P2X7R to interact with HSP90, therefore remains the most likely explanation for the change in I_1 amplitude.

Geldanamycin also alters apparent pore dilation, but not current facilitation. We studied the effect of geldanamycin on current facilitation and apparent pore dilation by measuring I_2 and the shift in the reversal potential of the ATP-gated current before and after application of the HSP90 antagonist. As shown in Fig. 6, geldanamycin significantly increased I_1 phase of the P2X7R current. In contrast, the total I_2 current, measured 60 sec after the start of the ATP application, wasn't significantly different in the presence and absence of geldanamycin (-253 ± 65 pA/pF and -239 ± 43 pA/pF, respectively). Similar effects were seen in the X2-X7-X7 chimera. We also measured a smaller shift in the reversal potential (~10 mV; Table 2) in the

Molecular Pharmacology Fast Forward. Published on June 14, 2016 as DOI: 10.1124/mol.115.102988
This article has not been copyedited and formatted. The final version may differ from this version.

presence of geldanamycin by comparison to measurements made in its absence (compare raw data of Figs. 4 and 7; Table 2). The fact that geldanamycin increases total current density but causes a smaller shift in the reversal potential of the ATP-gated current measured under bi-ionic $NMDG^+/Na^+$ conditions argues against the recent suggestion that the altered E_{rev} results entirely from an affect of ion accumulation (Li et al, 2015). Rather, the data support the ability of HSP90 to directly influence the ability of the P2X7R pore via C-terminus to adopt a conformational state with altered permeability to $NMDG^+$.

Inhibition of geldanamycin-potentiated I_1 current with deleted cysteine-rich juxtamembrane domain of P2X7R. Previous studies have shown that C-terminus of P2X7R involves the 18-amino acid cysteine-rich juxtamembrane domain contributed to current facilitation, apparent pore dilation and palmitoylation (Jiang et al, 2005; Yan et al, 2008; Gonnord et al, 2009; Yan et al, 2010; Roger et al, 2010). Resh (Resh, 2006) showed that palmitoylation can influence membrane binding of the modified proteins and the trafficking of ion channels. We thus investigated the effect of geldanamycin on ATP-induced currents using a deletion mutant (P2X7R[Δ18]) that lacks the 18-amino acid (362-379: CCRSRVYPSCKCCEPCAV) cysteine-rich site (Jiang et al, 2005). The ability of geldanamycin to potentiate the I_1 current in wild-type P2X7R completely disappeared in the truncated P2X7R[Δ18] (Fig. 8A). The same results were obtained using 17-AAG and 17-DMAG (Supplemental Fig. 1). Further, using Western blot analysis of protein expression, we saw no changes in total or surface P2X7R[Δ18] expression in the presence and absence of geldanamycin, 17-AAG and 17-DMAG (Fig. 9, Supplemental Fig. 2). In addition, I_2 current and the shift in the reversal potential in the presence and absence of geldanamycin was unchanged in P2X7R[Δ18]

Molecular Pharmacology Fast Forward. Published on June 14, 2016 as DOI: 10.1124/mol.115.102988
This article has not been copyedited and formatted. The final version may differ from this version.

(Fig. 8B-D). Taken together, these data suggest that HSP90 prevents facilitation of the initial ion influx by an action on the cysteine-rich domain of the C-terminus of the wild-type P2X7R.

Molecular Pharmacology Fast Forward. Published on June 14, 2016 as DOI: 10.1124/mol.115.102988
This article has not been copyedited and formatted. The final version may differ from this version.

Discussion

Site-directed mutagenesis of the C-terminus has numerous effects on P2XR channel function; amongst these, the best known is a change in the apparent ability of the pore to permeate large organic cations during long applications of ATP (Khakh et al, 1999; Egan et al, 2006; Erb et al, 2006; Yan et al, 2008; Yan et al, 2010). Further, the C-terminus has been shown to interact with a number of intracellular and cytoskeleton proteins, including HSP90 (Kim et al, 2001), in a manner that targets the receptor to the plasma membrane and regulates the gating of the P2X1R (Lalo et al, 2011; Lalo et al, 2012). In the present paper, we show that the HSP90 antagonist, geldanamycin, significantly changes the channel properties of the ATP-gated currents of a number of P2XRs (P2X2R, P2X4R, and P2X7R), suggesting that HSP90 indeed plays an important role in the regulation of P2XR function.

We took advantage of the fact that while both P2X2R and P2X7R show a change in the reversal potential of the ATP-gated currents measured under bi-ionic conditions during long applications of agonist, only the P2X7R shows current facilitation (Khakh et al, 1999; Yan et al, 2008; Yan et al, 2010). Although the structural bases of apparent pore dilation and current facilitation are unknown (but see below), it is tempting to speculate that functional differences in the P2X2R and the P2X7R arise from their divergent C-termini. Specifically, the C-terminus of the P2X7R is much longer than that of the P2X2R, and contains a distinct cysteine-rich domain (North, 2002). Truncated P2X7Rs that lack this domain fail to show pore dilation and current facilitation (Yan et al, 2008; Yan et al, 2010), suggesting that the C-terminus plays a pivotal role in producing these phenomena. Further, the cysteine-rich domain is absent in P2X2Rs that show clear changes in reversal potentials in response to prolonged applications of agonist, albeit at a

Molecular Pharmacology Fast Forward. Published on June 14, 2016 as DOI: 10.1124/mol.115.102988
This article has not been copyedited and formatted. The final version may differ from this version.

slower rate and to a lesser degree than the wild-type P2X7R (Khakh et al, 1999; Virginio et al, 1999; Yan et al, 2008; Mio et al, 2009; Yan et al, 2010; Khadra et al, 2012).

Using chimeric constructs of the P2X2R and P2X7R, we found that a full length P2X7R C-terminus is required to achieve the maximum degree of facilitation. That is, neither the chimeric P2X7Rs containing the C-terminus of P2X2R nor the truncated P2X7R[Δ18] show the same degree of facilitation as that seen in the full-length wild-type P2X7R. These engineered receptors also showed a smaller shift in the reversal potential during long applications of ATP, indicative of lesser apparent pore dilation. Recently, Li and coworkers (Li et al, 2015) suggested that the shift in equilibrium potential induced by prolonged P2X2 channel activation does not result from pore dilation, but rather from time-dependent alterations in the concentration of intracellular ions. However, our experiments clearly show that the geldanamycin decreased the shift in the reversal potential of the ATP-gated current measured under bi-ionic $NMDG^+/Na^+$ condition without effecting the ability of the long application of agonist to facilitate current amplitude. The smaller shift in the reversal potential paired to a larger inward current would seem to argue against an effect of ion accumulation. However, our data do not conclusively prove that HSP90 is capable of directing conformational changes in the P2X7R protein channel, and additional experiments derived from the study of Li and coworkers (Li et al, 2015) are needed to confidently rule out the possibility that a change in the intracellular concentrations of ions explains the effect of geldanamycin on the change in the reversal potential. While further experiments are clearly needed, our results suggest that C-terminal of the P2X7R, especially the cysteine-rich region, may regulate ion permeability by promoting the adoption of a unique open channel conformation.

Molecular Pharmacology Fast Forward. Published on June 14, 2016 as DOI: 10.1124/mol.115.102988
This article has not been copyedited and formatted. The final version may differ from this version.

We also found that the X2-X7-X7 chimera showed a decrease $NMDG^+$ permeability during long applications of ATP. In fact, this result is not surprising; others showed that mutating a highly conserved threonine (Thr^{15}) or non-conserved Serine (Ser^{23}) in the N-terminus of the rat P2X7R significantly alters $NMDG^+$ permeability (Yan et al, 2008) and ethidium bromide uptake (Allsopp et al, 2015). While it is tempting to speculate how the N- and C-terminus influences conformational states of the pore, firm determination awaits the solution of high-resolution structures of fully formed P2X7Rs.

P2X7Rs interact with a number of intracellular and membrane-spanning proteins (Kim et al, 2001; Gu et al, 2009). Adinolfi and coworkers (Adinolfi et al, 2003) used geldanamycin to show that tyrosine phosphorylation of HSP90 within the P2X7R complex negatively regulates channel function by lowering the affinity of the P2X7R for Bz-ATP through an action on a specific tyrosine (Tyr^{550}) in the C-terminal tail. In our study, we found that geldanamycin potentiated the initial I_1 component of the ATP-induced current of the wild-type P2X7R, while at the same time it inhibited the shift in the reversal potential. The potentiation of I_1 current by geldanamycin was not present in cells expressing the X7-X7-X2, X2-X7-X2 and P2X7R[Δ18] chimera. Further, pre-application of geldanamycin prevented the increase in $NMDG^+$ permeability in the wild-type receptor. All of these effects may reflect a constitutive action of HSP90 on P2X7R function as the result of an interaction with C-terminus. We do not think that geldanamycin exerts its effects by acting as an ATPase (Panaretou et al, 1998), because the broken-patch method we use to record membrane current is expected remove unbound intracellular ATP by dilution of the cytoplasm with the contents of the recording pipette, thereby effectively making the action of an ATPase redundant. Rather, geldanamycin may act to displace ATP from a critical binding site.

Molecular Pharmacology Fast Forward. Published on June 14, 2016 as DOI: 10.1124/mol.115.102988
This article has not been copyedited and formatted. The final version may differ from this version.

Further experiments are needed to more precisely define the action of geldanamycin at the molecular level. Nevertheless, out data clearly show that C-terminus of the P2X7R is somehow involved in geldanamycin effect. This should not be surprising because several reports highlight the importance of this domain in regulation of channel function. For example, Smart and coworkers (Smart et al, 2003) showed that the distal C-terminal domain regulates surface expression of the P2X7R and is essential for the apparent pore dilation and current facilitation reported here. Further, separate domains within the C-terminus contribute to the Ca^{2+} dependent (Rogers et al, 2008; Yan et al, 2011) and independent (Roger et al, 2010) components of current facilitation of the P2X7R. Moreover, Gonnord and coworkers (Gonnord et al, 2009) have indicated that the cysteine-rich site is important for the P2X7 palmitoylation that plays a critical role in the association with the lipid microdomains of plasma membrane. Now, our work with wild-type and chimeric receptors suggest the HSP90 facilitates P2X7R current through a physical interaction with the the juxtamembrane cysteine-rich domain. However, how HSP90 causes facilitation is unknown. One possibility is that the binding of HSP90 at or near the cysteine-rich domain bends the C-terminus into a unique conformation that is capable of changing channel kinetics in a way that promotes $NMDG^{+}$ permeability. Again, proof of this hypothesis awaits the arrival of full length, high resolution structures in complex with HSP90.

Ample data suggest that the C-terminus plays a significantly role in the regulation of inflammatory response (Adriouch et al, 2002), apoptosis (Wiley et al, 2002; Le et al, 2004; Feng et al, 2006) and pain (Sorge et al, 2012) by the P2X7R. Our experiments extend this work and suggest that one role for the C-terminus is to act as an interaction site for an accessory regulatory protein, HSP90. If so, then drugs that modulate the binding of HSP90 to the C-terminus may be

Molecular Pharmacology Fast Forward. Published on June 14, 2016 as DOI: 10.1124/mol.115.102988
This article has not been copyedited and formatted. The final version may differ from this version.

useful therapies for neuropathic pain, apoptosis, and inflammation.

Molecular Pharmacology Fast Forward. Published on June 14, 2016 as DOI: 10.1124/mol.115.102988
This article has not been copyedited and formatted. The final version may differ from this version.

Acknowledgements

The authors are thankful to Shiwori Osanai for technical assistance.

Authorship Contributions

Participated in research design: Migita

Conducted experiments: Migita, Shimoyama

Performed data analysis: Migita, Shimoyama

Wrote or contributed to the writing of the manuscript: Migita, Egan, Ozaki, Shimoyama, Yamada, Nikaido, Furukawa, Shiba, Ueno

Molecular Pharmacology Fast Forward. Published on June 14, 2016 as DOI: 10.1124/mol.115.102988
This article has not been copyedited and formatted. The final version may differ from this version.

References

Adinolfi E, Kim M, Young MT, Di Virgilio F, and Surprenant A (2003) Tyrosine phosphorylation of HSP90 within the P2X7 receptor complex negatively regulates P2X7 receptors. *J Biol Chem* **278**: 37344-37351.

Adriouch S, Dox C, Welge V, Seman M, Koch-Nolte F, and Haag F (2002) Cutting edge: a natural P451L mutation in the cytoplasmic domain impairs the function of the mouse P2X7 receptor. *J Immunol* **169**: 4108-4112.

Allsopp RC and Evans RJ (2015) Contribution of the Juxtatransmembrane Intracellular Regions to the Time Course and Permeation of ATP-gated P2X7 Receptor Ion Channels. *J Biol Chem* **290**: 14556-14566.

Barrera NP, Ormond SJ, Henderson RM, Murrell-Lagnado RD, and Edwardson JM (2005) Atomic force microscopy imaging demonstrates that P2X2 receptors are trimers but that P2X6 receptor subunits do not oligomerize. *J Biol Chem* **280**: 10759-10765.

Chen H, Xia Y, Fang D, Hawke D, and Lu Z (2009) Caspase-10-mediated heat shock protein 90 beta cleavage promotes UVB irradiation-induced cell apoptosis. *Mol Cell Biol* **29:** 3657-3664.

Coddou C, Yan Z, and Stojilkovic SS (2015) Role of domain calcium in purinergic P2X2 receptor channel desensitization. *Am J Physiol Cell Physiol* **308:** C729-736.

Costa-Junior HM, Sarmento Vieira F, and Coutinho-Silva R (2011) C terminus of the P2X7 receptor: treasure hunting. *Purinergic Signal* **7**: 7-19.

Egan TM, Cox JA, and Voigt MM (2004) Molecular structure of P2X receptors. *Curr Top Med Chem* **4**: 821-829.

Egan TM, Samways DS, and Li Z (2006) Biophysics of P2X receptors. *Pflugers Arch* **452**: 501-512.

Erb L, Liao Z, Seye CI, and Weisman GA (2006) P2 receptors: intracellular signaling. *Pflugers Arch* **452**: 552-562.

Feng YH, Li X, Zeng R, and Gorodeski GI (2006) Endogenously expressed truncated P2X7 receptor lacking the C-terminus is preferentially upregulated in epithelial cancer cells and fails to mediate ligand-induced pore formation and apoptosis. *Nucleosides Nucleotides Nucleic Acids* **25**: 1271-1276.

Gonnord P, Delarasse C, Auger R, Benihoud K, Prigent M, Cuif MH, Lamaze C, and Kanellopoulos JM (2009) Palmitoylation of the P2X7 receptor, an ATP-gated channel, controls its expression and association with lipid rafts. *FASEB J* **23**: 795-805.

Gu BJ, Rathsam C, Stokes L, McGeachie AB, and Wiley JS (2009) Extracellular ATP dissociates nonmuscle myosin from P2X7 complex: this dissociation regulates P2X7 pore formation. *Am J Physiol Cell Physiol* **297**: C430–C439.

Hattori M and Gouaux E (2012) Molecular mechanism of ATP binding and ion channel activation in P2X receptors. *Nature* **485**: 207-212.

Jiang LH, Rassendren F, Mackenzie A, Zhang YH, Surprenant A, and North RA (2005) N-methyl-D-glucamine and propidium dyes utilize different permeation pathways at rat P2X7 receptors. *Am J Physiol Cell Physiol* **289**: C1295-1302.

Kawate T, Michel JC, Birdsong WT, and Gouaux E (2009) Crystal structure of the ATP-gated P2X4 ion channel in the closed state. *Nature* **460**: 592-598.

Khadra A, Yan Z, Coddou C, Tomić M, Sherman A, and Stojilkovic SS (2012) Gating properties of the P2X2a and P2X2b receptor channels: experiments and mathematical modeling. *J Gen Physiol* **139**: 333-348.

Khadra A, Tomić M, Yan Z, Zemkova H, Sherman A, and Stojilkovic SS (2013) Dual gating mechanism and function of P2X7 receptor channels. *Biophys J* **104**: 2612-2621.

Khakh BS, Bao XR, Labarca C, and Lester HA (1999) Neuronal P2X transmitter-gated cation channels change their ion selectivity in seconds. *Nat Neurosci* **2**: 322-330.

Kim M, Jiang LH, Wilson HL, North RA, and Surprenant A (2001) Proteomic and functional evidence for a P2X7 receptor signaling complex. *EMBO J* **20**: 6347–6358.

Lalo U, Roberts JA, and Evans RJ (2011) Identification of human P2X1 receptor-interacting proteins reveals a role of the cytoskeleton in receptor regulation. *J Biol Chem* **286**: 30591-30599.

Lalo U, Jones S, Roberts JA, Mahaut-Smith MP, and Evans RJ (2012) Heat shock protein 90 inhibitors reduce trafficking of ATP-gated P2X1 receptors and human platelet responsiveness. *J Biol Chem* **287**: 32747-32754.

Le Stunff H, Auger R, Kanellopoulos J, and Raymond MN (2004) The Pro-451 to Leu polymorphism within the C-terminal tail of P2X7 receptor impairs cell death but not phospholipase D activation in murine thymocytes. *J Biol Chem* **279**: 16918-16926.

Levin TC, Wickliffe KE, Leppla SH, and Moayeri M (2008) Heat shock inhibits caspase-1 activity while also preventing its inflammasome-mediated activation by anthrax lethal toxin. *Cell Microbiol* **10**: 2434-2446.

Li M, Toombes GE, Silberberg SD, and Swartz KJ (2015) Physical basis of apparent pore dilation of ATP-activated P2X receptor channels. *Nat Neurosci* **18**: 1577-1583.

Liang X, Samways DS, Wolf K, Bowles EA, Richards JP, Bruno J, Dutertre S, DiPaolo RJ, and Egan TM (2015) Quantifying Ca2+ current and permeability in ATP-gated P2X7 receptors. *J Biol Chem* **290**: 7930-7942.

Migita K, Haines WR, Voigt MM, and Egan TM (2001) Polar residues of the second transmembrane domain influence cation permeability of the ATP-gated P2X2 receptor. *J Biol Chem* **276**: 30934-30941.

Mio K, Ogura T, Yamamoto T, Hiroaki Y, Fujiyoshi Y, Kubo Y, and Sato C (2009) Reconstruction of the P2X2 receptor reveals a vase-shaped structure with lateral tunnels above the membrane. *Structure* **17**: 266-275.

Nicke A, Baumert HG, Rettinger J, Eichele A, Lambrecht G, Mutschler E, and Schmalzing G (1998) P2X1 and P2X3 receptors form stable trimers: a novel structural motif of ligand-gated ion channels. *EMBO J* **17**: 3016–3028.

North RA (2002) Molecular physiology of P2X receptors. *Physiol Rev* **82**: 1013-1067.

Panaretou B, Prodromou C, Roe SM, O'Brien R, Ladbury JE, Piper PW, and Pearl LH (1998) ATP binding and hydrolysis are essential to the function of the Hsp90 molecular chaperone in vivo. *EMBO J* **17:** 4829-4836.

Resh MD (2006) Palmitoylation of ligands, receptors, and intracellular signaling molecules. *Sci STKE* **359**: re14.

Roger S, Pelegrin P, and Surprenant A (2008) Facilitation of P2X7 receptor currents and membrane blebbing via constitutive and dynamic calmodulin binding. *J Neurosci* **28**: 6393-6401.

Roger S, Gillet L, Baroja-Mazo A, Surprenant A, and Pelegrin P (2010) C-terminal calmodulin-binding motif differentially controls human and rat P2X7 receptor current facilitation. *J Biol Chem* **285**: 17514-17524.

Rokic MB and Stojilkovic SS (2013) Two open states of P2X receptor channels. *Front Cell Neurosci* **7**: 215.

Smart ML, Gu B, Panchal RG, Wiley J, Cromer B, Williams DA, and Petrou S (2003) P2X7 receptor cell surface expression and cytolytic pore formation are regulated by a distal C-terminal region. *J Biol Chem* **278**: 8853-8860.

Sorge RE, Trang T, Dorfman R, Smith SB, Beggs S, Ritchie J, Austin JS, Zaykin DV, Vander Meulen H, Costigan M, Herbert TA, Yarkoni-Abitbul M, Tichauer D, Livneh J, Gershon E, Zheng M, Tan K, John SL, Slade GD, Jordan J, Woolf CJ, Peltz G, Maixner W, Diatchenko L, Seltzer Z, Salter MW, and Mogil JS (2012) Genetically determined P2X7 receptor pore formation regulates variability in chronic pain sensitivity. *Nat Med* **18**: 595-599.

Surprenant A, Rassendren F, Kawashima E, North RA, and Buell G (1996) The cytolytic P2Z receptor for extracellular ATP identified as a P2X receptor (P2X7). *Science* **272**: 735-738.

Virginio C, Mackenzie A, Rassendren FA, North RA, and Surprenant A (1999) Pore dilation of neuronal P2X receptor channels. *Nat Neurosci* **2**: 315–321.

Wiley JS, Dao-Ung LP, Gu BJ, Sluyter R, Shemon AN, Li C, Taper J, Gallo J, and Manoharan A (2002) A loss-of-function polymorphic mutation in the cytolytic P2X7 receptor gene and chronic lymphocytic leukaemia: a molecular study. *Lancet* **359**: 1114-1119.

Yan Z, Li S, Liang Z, Tomić M, and Stojilkovic SS (2008) The P2X7 receptor channel pore dilates under physiological ion conditions. *J Gen Physiol* **132**: 563-573.

Yan Z, Khadra A, Li S, Tomić M, Sherman A, and Stojilkovic SS (2010) Experimental characterization and mathematical modeling of P2X7 receptor channel gating. *J Neurosci* **30**: 14213-14224.

Yan Z, Khadra A, Sherman A, and Stojilkovic SS (2011) Calcium-dependent block of P2X7 receptor channel function is allosteric. *J Gen Physiol* **138**: 437-452.

Molecular Pharmacology Fast Forward. Published on June 14, 2016 as DOI: 10.1124/mol.115.102988
This article has not been copyedited and formatted. The final version may differ from this version.

Footnotes

This work was supported by Grant-in-Aid for Scientific Research (C) [NO. 26460693] and for Exploratory Research [NO. 25670663] from Japan Society for the Promotion of Science and by Priority Research Grant for Young Scientists Designated by the President of Hirosaki University.

Molecular Pharmacology Fast Forward. Published on June 14, 2016 as DOI: 10.1124/mol.115.102988
This article has not been copyedited and formatted. The final version may differ from this version.

Figure Legends

Figure 1. Effect of the HSP90 inhibitor geldanamycin on other P2XRs-mediated currents. A, representative currents evoked by 30 μM ATP for P2X2R, P2X3R and P2X4R or 3 mM ATP for P2X7R in the absence (upper figures) or presence (lower figures) of 5 μM geldanamycin (20 min). B, mean ratio showed 2nd ATP currents in the absence (black bar) or presence (white bar) of geldanamycin divide by 1st ATP current in P2XRs (n = 4-6). *P < 0.05, **P < 0.01 compared with the corresponding values from the absence of geldanamycin (Student's t-test).

Figure 2. Property of P2X7 chimeras. A, schematic representations of the wild-type and chimeric receptors used in this study. B, immunofluorescence staining of wild-type and chimeric receptors in HEK-293T cells transiently expressing these receptors.

Figure 3. P2X7 and its chimeras receptors currents during long-term stimulation with ATP. Representative traces showing the whole cell currents elicited by a 60-s application of 3 mM ATP for P2X7 and its chimeras receptors and 30 μM ATP for P2X2R. Dotted line indicates bottom of current under the presence of ATP.

Figure 4. Permeability to $NMDG^+$ in P2X7 and its chimeras receptors. Voltage ramps of -80 mV to 40 mV were applied to the cells during 60 sec activation of P2X7R and its mutants by 3 mM ATP or P2X2R by 30 μM ATP in extracellular $NMDG^+$. The currents initially (1 sec) show a low permeability to $NMDG^+$ that is followed by a progressive rightward-shift in the reversal potential of the ATP-activated current in

P2X7 and P2X2Rs.

Figure 5. Effect of the HSP90 inhibitor geldanamycin on P2X7 and its chimeras receptors-mediated currents. A, representative currents evoked by 3 mM ATP recorded in cells expressing P2X7R and its chimeras receptors or 30 μM ATP in P2X2R in the absence or presence of 5 μM geldanamycin (20 min). B, mean normalized data of P2X7 and its chimeras receptors-mediated 3 mM ATP currents in normal HEPES solution and in the presence of 5 μM geldanamycin. (n = 4-8). Statistical analysis was performed by one-way ANOVA followed by Tukey's test (**P < 0.01).

Figure 6. Effect of geldanamycin on current facilitation in P2X7R and its mutants. Representative traces showing the whole cell currents elicited by a 60 sec application of 3 mM ATP for P2X7R in the presence and absence of 5 μM geldanamycin (20 min).

Figure 7. Effect of geldanamycin on permeability to $NMDG^+$ in P2X7R and its mutants. Voltage ramps of -80 mV to 40 mV were applied to the cells during 60 sec activation of P2X7R by 3 mM ATP in extracellular $NMDG^+$ under the presence of 5 μM geldanamycin (20 min).

Figure 8. Effect of geldanamycin on ATP-induced currents in P2X7R[Δ18]. A, representative currents evoked by 3 mM ATP recorded in cells expressing P2X7R and P2X7R[Δ18] in the absence or presence of 5 μM geldanamycin (20 min). Mean normalized data of P2X7 and P2X7R[Δ18]-mediated 3 mM ATP currents in normal HEPES solution and in the presence of 5 μM geldanamycin (n = 4-8). Statistical analysis was performed by one-way ANOVA followed by Tukey's test (**P < 0.01). B, representative

traces showing the whole cell currents elicited by a 60 sec application of 3 mM ATP for P2X7R[Δ18] in the presence and absence of 5 μM geldanamycin (20 min). C, Voltage ramps of -80 mV to 40 mV were applied to the cells during 60 sec activation of P2X7R[Δ18] by 3 mM ATP in extracellular $NMDG^+$. D, Voltage ramps of -80 mV to 40 mV were applied to the cells during 60 sec activation of P2X7R[Δ18] by 3 mM ATP in extracellular $NMDG^+$ under the presence of 5 μM geldanamycin (20 min).

Figure 9. Effect of geldanamycin on P2X7R and P2X7R[Δ18] expression. A, Western Blots showing total or plasma membrane of P2X7R, P2X7R[Δ18], HSP90, GAPDH and β-actin proteins in HEK293T cells transfected with P2X7R (X7) and P2X7R[Δ18] (Δ18) treated or untreated with 5 μM geldanamycin for 20 min. B, summary of the amount of P2X7R and P2X7R[Δ18] relative to β-actin. Data indicate no difference in the total (n = 6) or surface (n = 3) level of P2X7R, P2X7R[Δ18] and HSP90 between treated and untreated with geldanamycin.

Molecular Pharmacology Fast Forward. Published on June 14, 2016 as DOI: 10.1124/mol.115.102988
This article has not been copyedited and formatted. The final version may differ from this version.

Table 1

60 sec application of ATP in P2X7 chimeras

Chimera	10-90% Rise time (ms)	decay time constant (ms)	I_1 (pA/pF)	I_2 (pA/pF)	n
X7-X7-X7	32 ± 3	252 ± 27	-102 ± 31	-213 ± 56	8
X2-X7-X7	38 ± 6	833 ± 200	-247 ± 38	-425 ± 30*	6
X7-X7-X2	81 ± 15**	945 ± 204	-11 ± 4	-9 ± 3*	5
X2-X7-X2	44 ± 5	187 ± 24	-333 ± 126	-124 ± 42	6
X7[Δ18]	54 ± 5	1439 ± 603**	-124 ± 37	-95 ± 40	5
X2-X2-X2	97 ± 7**	121 ± 22	-1212 ± 299**	-195 ± 96	4

I_1: initial peak current; I_2: inward current at 60 sec; nd is not determined
Value are mean ± SEM; n: number of experiments;
*$P < 0.05$, **$P < 0.01$ vs wild-type P2X7 (Tukey's test)*

Molecular Pharmacology Fast Forward. Published on June 14, 2016 as DOI: 10.1124/mol.115.102988
This article has not been copyedited and formatted. The final version may differ from this version.

Table 2

Permeability of the wild-type P2X7R and its mutants to $NMDG^+$

Chimera	E_{rev} (mV)		Δv_{rev} (mV)	P_{NMDG}/P_{Cs}		n
	1 sec	60 sec		1 sec	60 sec	
X7-X7-X7	-38.9 ± 1.7	-13.0 ± 5.9[b]	25.9 ± 5.7	0.21 ± 0.01	0.67 ± 0.12[b]	6
+ geldanamycin	-39.4 ± 3.0	-31.9 ± 2.7[a']	7.7 ± 1.2[a]	0.22 ± 0.03	0.29 ± 0.04[a]	7
X2-X7-X7	-45.4 ± 1.1	-35.9 ± 1.4[ab]	9.5 ± 1.7[a]	0.17 ± 0.01	0.24 ± 0.01[a]	5
+ geldanamycin	-39.1 ± 0.6	-34.9 ± 2.1[a]	4.3 ± 2.0[a]	0.21 ± 0.01	0.26 ± 0.02[a]	7
X7-X7-X2	-41.8 ± 7.3	-39.4 ± 6.6[a]	2.4 ± 2.5[a]	0.23 ± 0.07	0.25 ± 0.06[a]	6
+ geldanamycin	-42.5 ± 2.0	-43.2 ± 2.9[a]	2.6 ± 2.0[a]	0.19 ± 0.02	0.19 ± 0.02[a]	5
X2-X7-X2	-46.6 ± 3.9	-39.5 ± 6.5[a]	8.8 ± 2.3[a]	0.16 ± 0.02	0.24 ± 0.05[a]	6
+ geldanamycin	-37.6 ± 2.0	-37.4 ± 3.5[a]	1.3 ± 1.7[a]	0.23 ± 0.02	0.24 ± 0.03[a]	5
X7[Δ18]	-33.5 ± 2.0	-33.5 ± 1.0[a']	2.1 ± 0.9[a]	0.27 ± 0.02	0.27 ± 0.01[a]	6
+ geldanamycin	-31.5 ± 1.5	-35.1 ± 3.4[a]	-3.6 ± 2.6[a]	0.29 ± 0.02	0.26 ± 0.04[a]	5
X2-X2-X2	-47.9 ± 1.0	-32.6 ± 2.4[a'b]	15.8 ± 5.3	0.15 ± 0.01	0.28 ± 0.03[ab]	6

Reversal potential (Erev) and relative permeability (P_{NMDG}/P_{Cs}) for wild-type P2X7R and its chimeraes at the beginning (1sec) and end (60 sec) of 60 sec application of ATP.
Value are mean ± SEM; n: number of experiments;
Significant differences between wild-type P2X7R and others; [a']$P < 0.05$, [a]$P < 0.01$ *(Tukey's test)*
Significant shifts between 1 sec and 60 sec; [b']$P < 0.05$, [b]$P < 0.01$ *(Student's t-test)*

Molecular Pharmacology Fast Forward. Published on June 14, 2016 as DOI: 10.1124/mol.115.102988
This article has not been copyedited and formatted. The final version may differ from this version.

Table 3

Effect of geldanamycin on current facilitation evoked by 60 sec application of ATP in wild-type P2X7R and and its mutants

Chimera	I_1 (pA/pF)	I_2 (pA/pF)	$I_1/I_{control}$	$I_2/I_{control}$	n
X7-X7-X7	-110 ± 24	-239 ± 43	0.9 ± 0.0	2.4 ± 0.4	14
+ geldanamycin	-198 ± 45	-253 ± 65	2.1 ± 0.5*	2.5 ± 0.4	11
X2-X7-X7	-474 ± 194	-650 ± 232	0.7 ± 0.1	1.0 ± 0.1	5
+ geldanamycin	-427 ± 121	-557 ± 117	1.0 ± 0.1	1.4 ± 0.2	5
X7-X7-X2	-2 ± 1	-1 ± 1	0.8 ± 0.4	0.4 ± 0.2	3
+ geldanamycin	-5 ± 2	-4 ± 1	1.1 ± 0.0	0.7 ± 0.1	3
X2-X7-X2	-74 ± 34	-18 ± 8	0.5 ± 0.2	0.1 ± 0.0	6
+ geldanamycin	-273 ± 108	-56 ± 17	0.5 ± 0.1	0.1 ± 0.0	3
X7[Δ18]	-101 ± 25	-78 ± 26	0.8 ± 0.1	0.6 ± 0.1	8
+ geldanamycin	-278 ± 89	-188 ± 66	0.7 ± 0.1	0.5 ± 0.1	4

Value are mean ± SEM; n: number of experiments;
**P < 0.05, **P < 0.01 vs Normal solution (Student's t-test)*

Molecular Pharmacology Fast Forward. Published on June 14, 2016 as DOI: 10.1124/mol.115.102988
This article has not been copyedited and formatted. The final version may differ from this version.

Table 4

ATP pharmacology of P2X7 chimeras

Chimera	EC_{50} (μM)	Hill coefficient	n
X7-X7-X7	1473 ± 40	1.7	12
X7-X7-X7 (geld)	1377 ± 253	5.4	7
X2-X7-X7	574 ± 22**	1.9	6
X7-X7-X2	304 ± 90**	0.9	5
X2-X7-X2	543 ± 40**	2.0	6
X7[Δ18]	265 ± 51**	0.9	5
X7[Δ18] (geld)	480 ± 197**	1.1	8
X2-X2-X2	13 ± 0**	3.4	7

geld: geldanamycin; Value are mean ± SEM; n: number of experiments;
***P < 0.01 vs wild-type P2X7 (Tukey's test)*

Molecular Pharmacology Fast Forward. Published on June 14, 2016 as DOI: 10.1124/mol.115.102988
This article has not been copyedited and formatted. The final version may differ from this version.

Figure 1

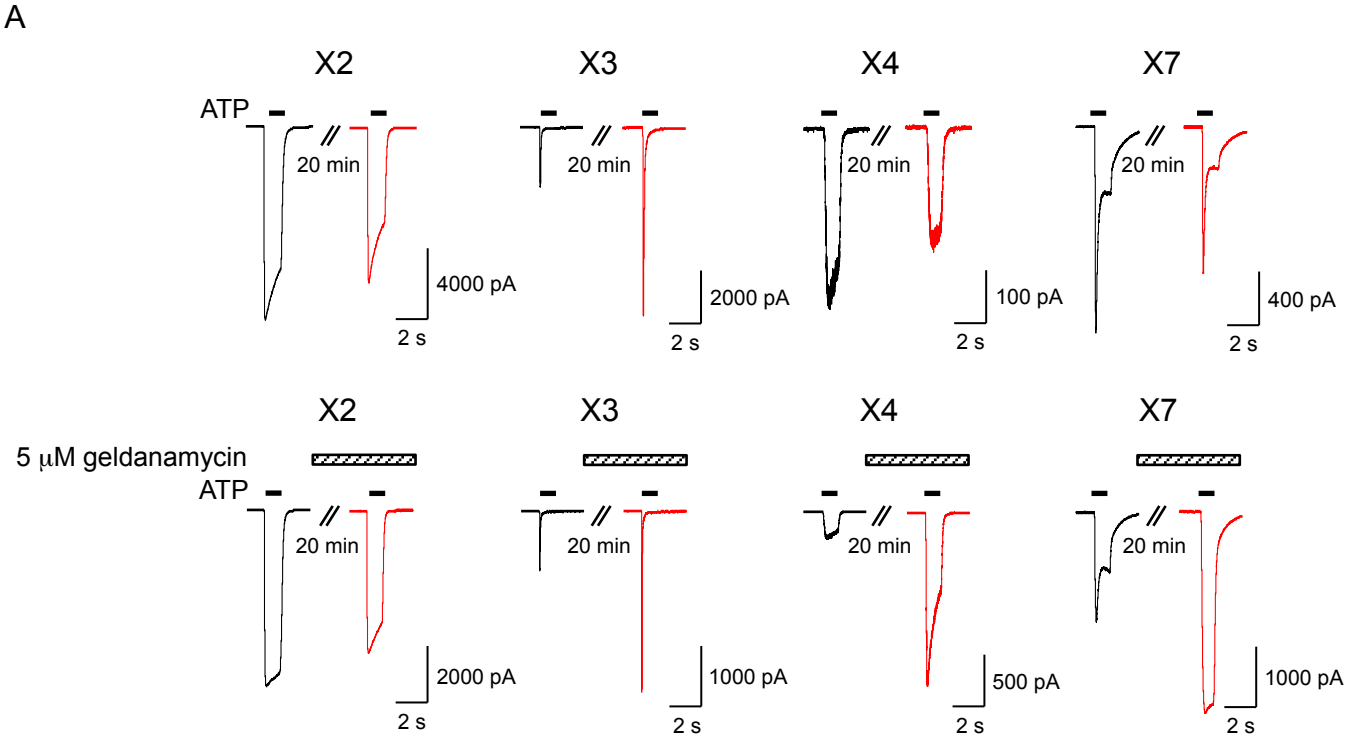

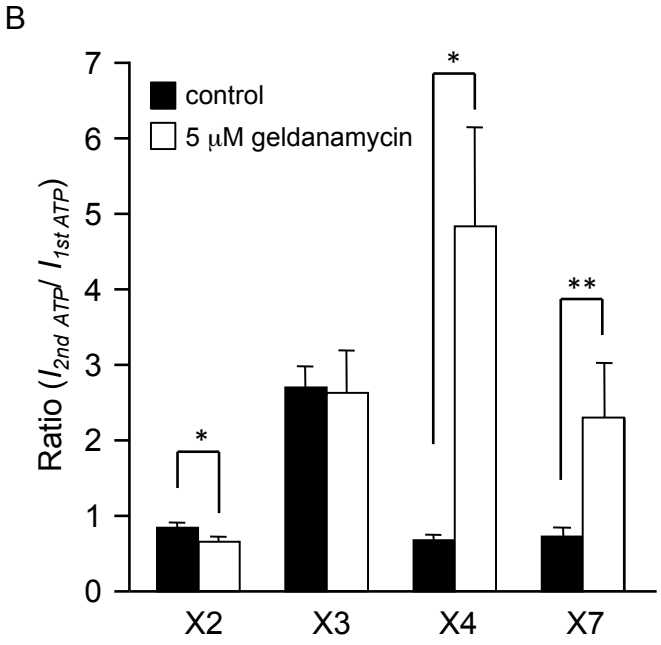

Figure 2

A

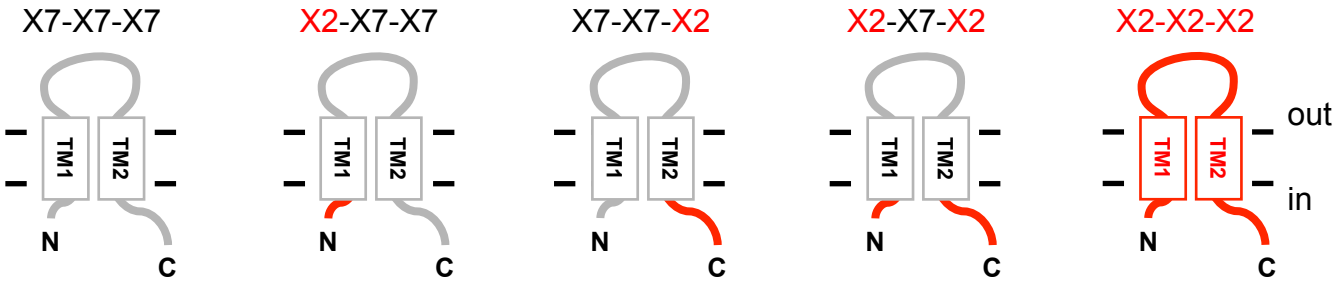
X7-X7-X7
X2-X7-X7
X7-X7-X2
X2-X7-X2
X2-X2-X2
TM1
TM2
N
C
out
in

B

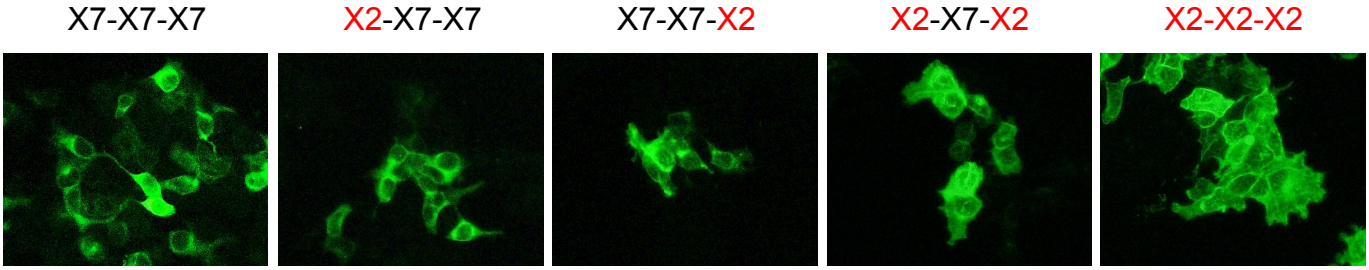
X7-X7-X7
X2-X7-X7
X7-X7-X2
X2-X7-X2
X2-X2-X2

Figure 3

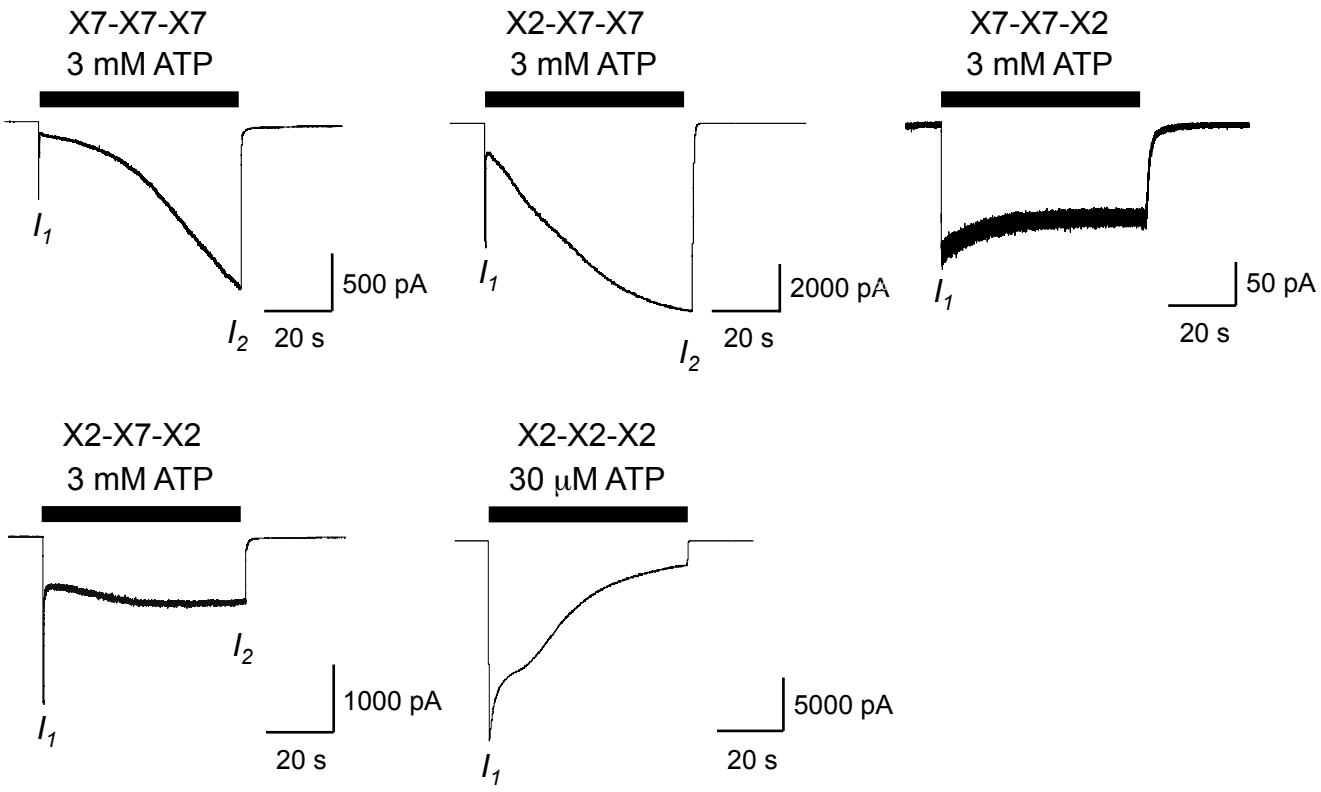
X7-X7-X7
3 mM ATP
I1
I2
500 pA
20 s
X2-X7-X7
3 mM ATP
I1
I2
2000 pA
20 s
X7-X7-X2
3 mM ATP
I1
50 pA
20 s
X2-X7-X2
3 mM ATP
I2
I1
1000 pA
20 s
X2-X2-X2
30 μM ATP
I1
5000 pA
20 s

Figure 4

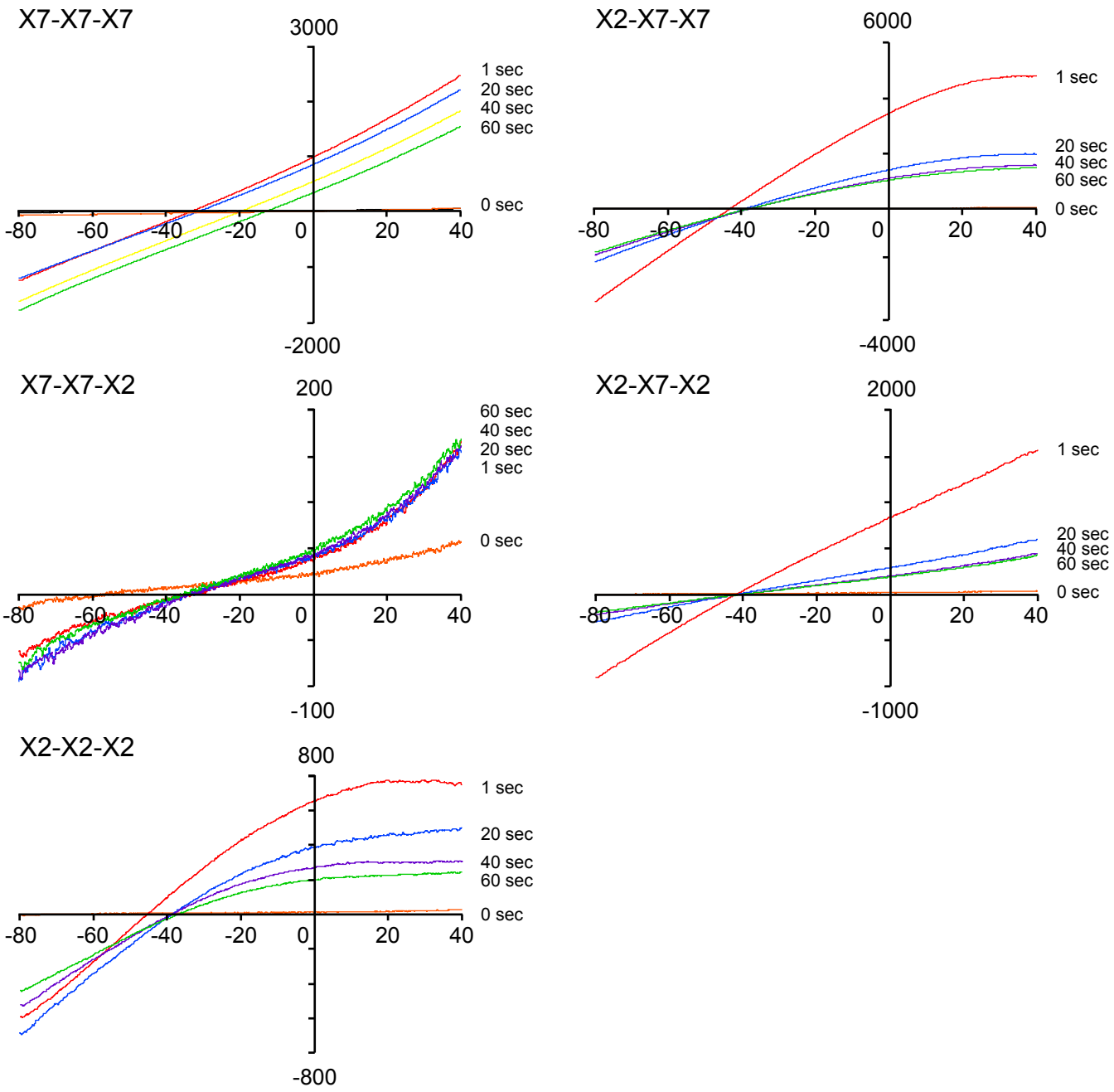
X7-X7-X7
3000
1 sec
20 sec
40 sec
60 sec
0 sec
-80
-60
-40
-20
0
20
40
-2000
X2-X7-X7
6000
1 sec
20 sec
40 sec
60 sec
0 sec
-4000
X7-X7-X2
200
60 sec
40 sec
20 sec
1 sec
0 sec
-100
X2-X7-X2
2000
1 sec
20 sec
40 sec
60 sec
0 sec
-1000
X2-X2-X2
800
1 sec
20 sec
40 sec
60 sec
0 sec
-800

Figure 5

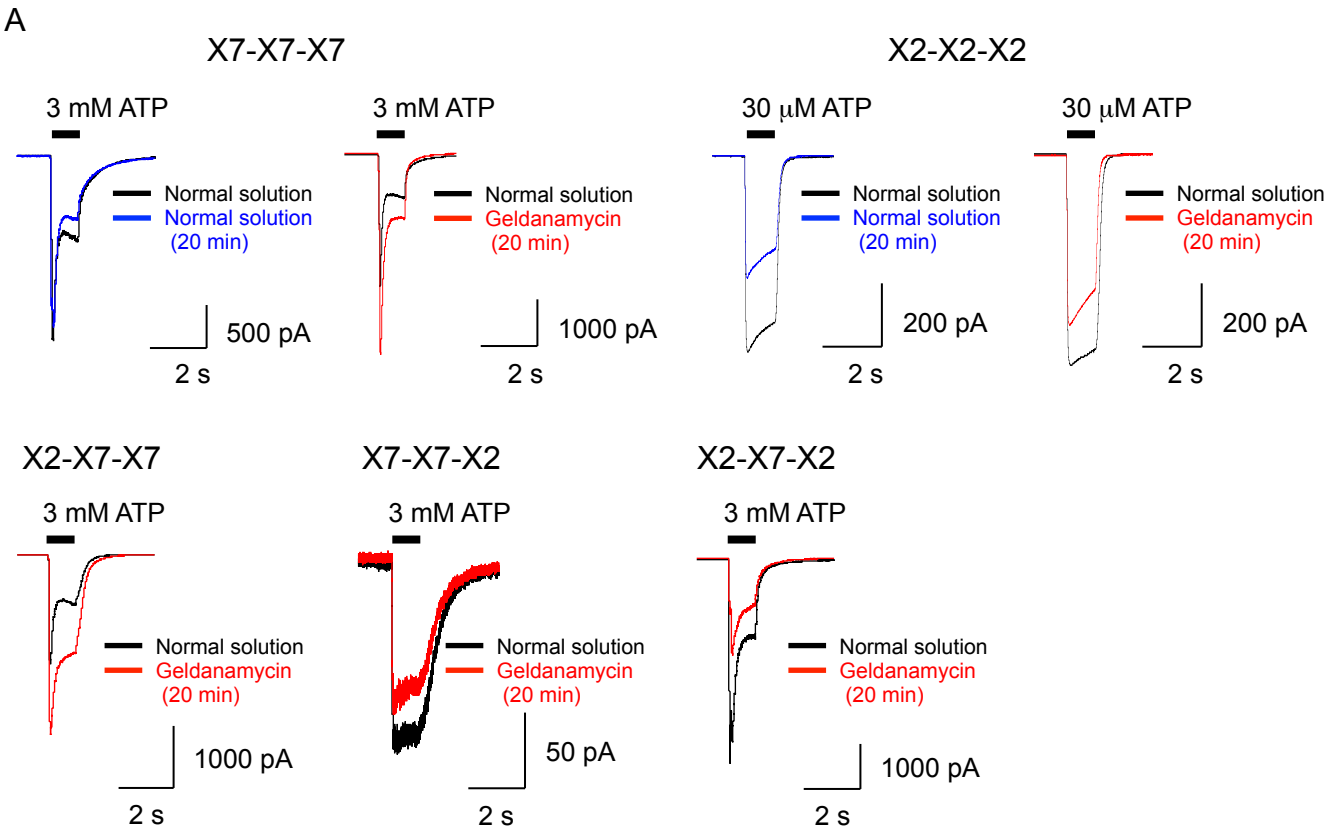
A
X7-X7-X7
X2-X2-X2
3 mM ATP
30 μM ATP
Normal solution
Normal solution
(20 min)
Geldanamycin
(20 min)
500 pA
1000 pA
200 pA
2 s
X2-X7-X7
X7-X7-X2
X2-X7-X2
50 pA

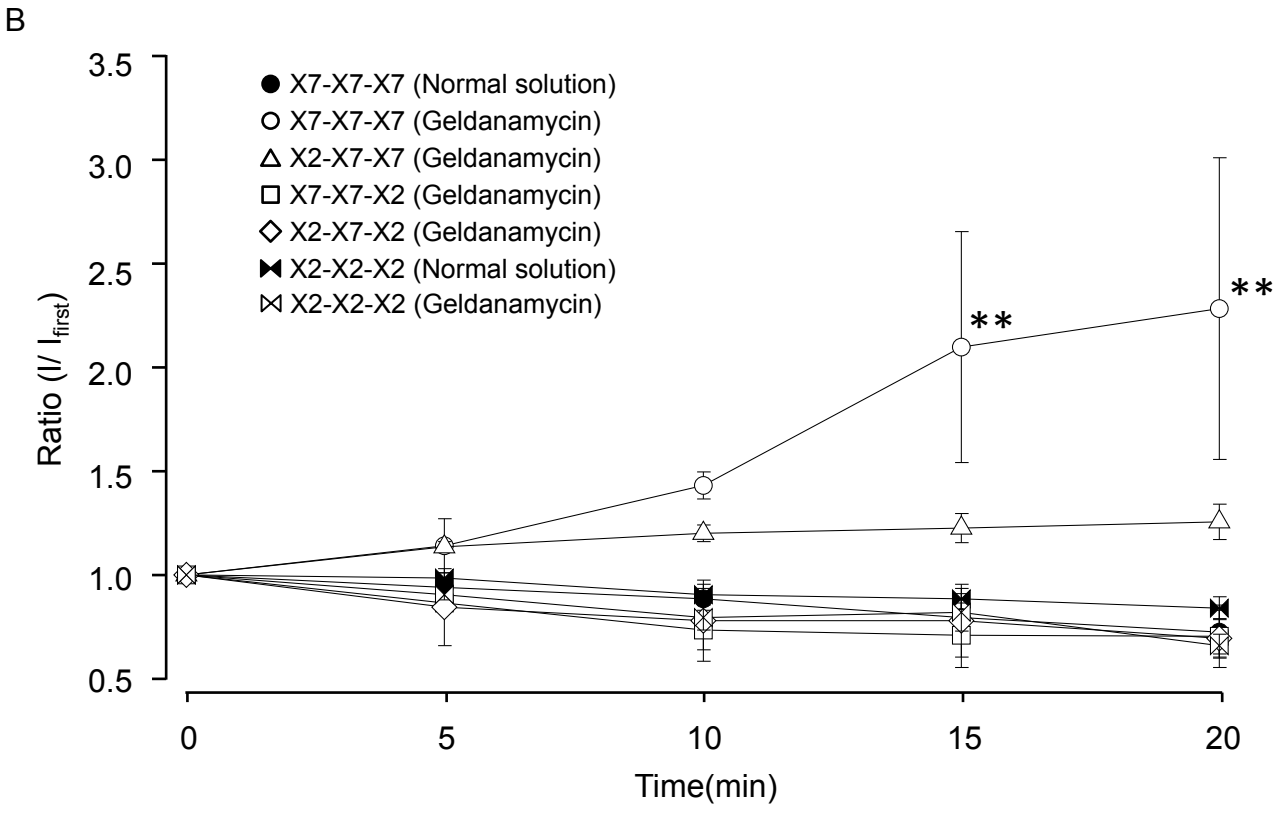
B
X7-X7-X7 (Normal solution)
X7-X7-X7 (Geldanamycin)
X2-X7-X7 (Geldanamycin)
X7-X7-X2 (Geldanamycin)
X2-X7-X2 (Geldanamycin)
X2-X2-X2 (Normal solution)
X2-X2-X2 (Geldanamycin)
Ratio (I/ I first)
Time(min)
**
**

Figure 6

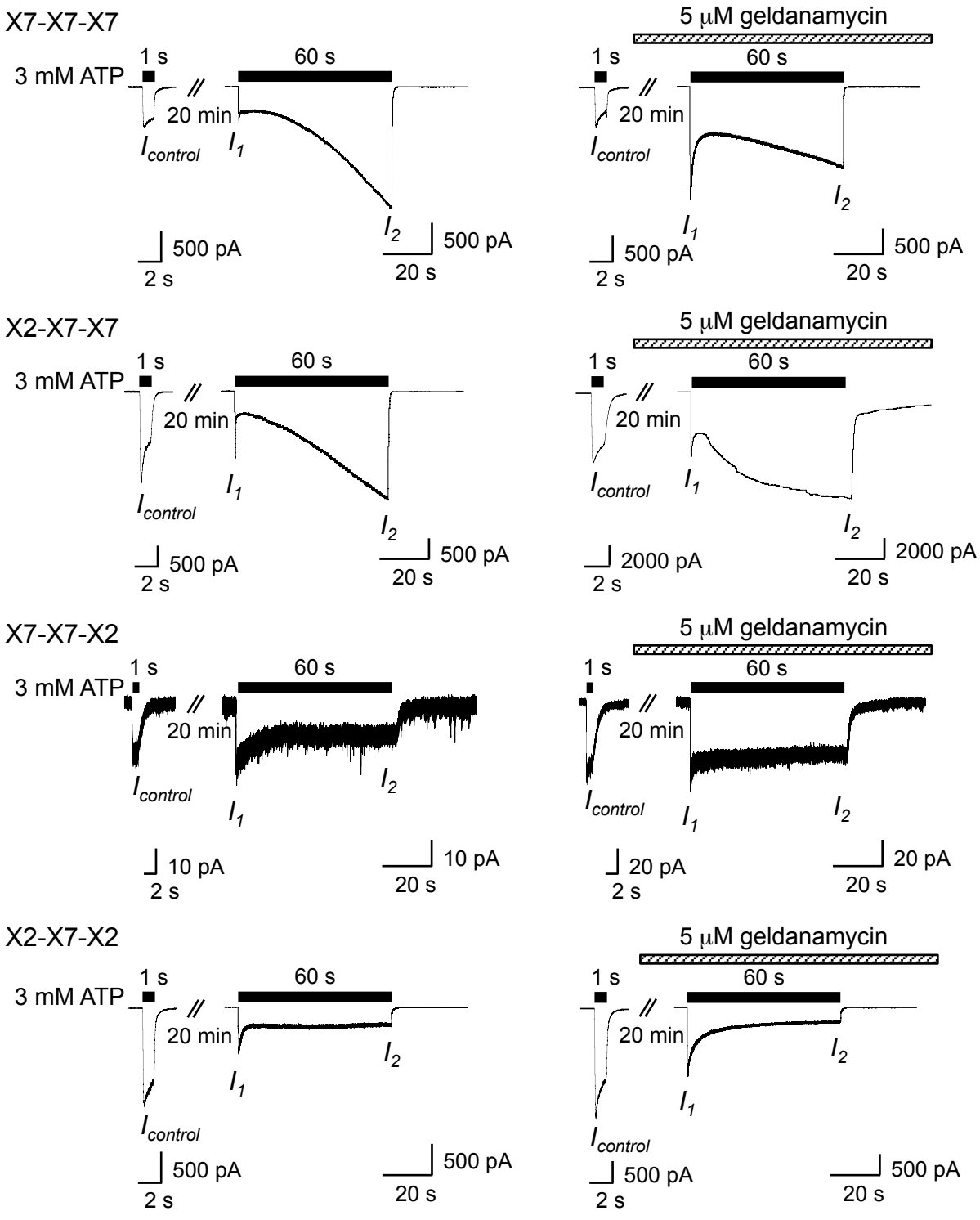
X7-X7-X7
3 mM ATP
1 s
60 s
20 min
$I_{control}$
I_1
I_2
500 pA
2 s
500 pA
20 s
5 μM geldanamycin
X2-X7-X7
2000 pA
X7-X7-X2
10 pA
20 pA
X2-X7-X2

Figure 7

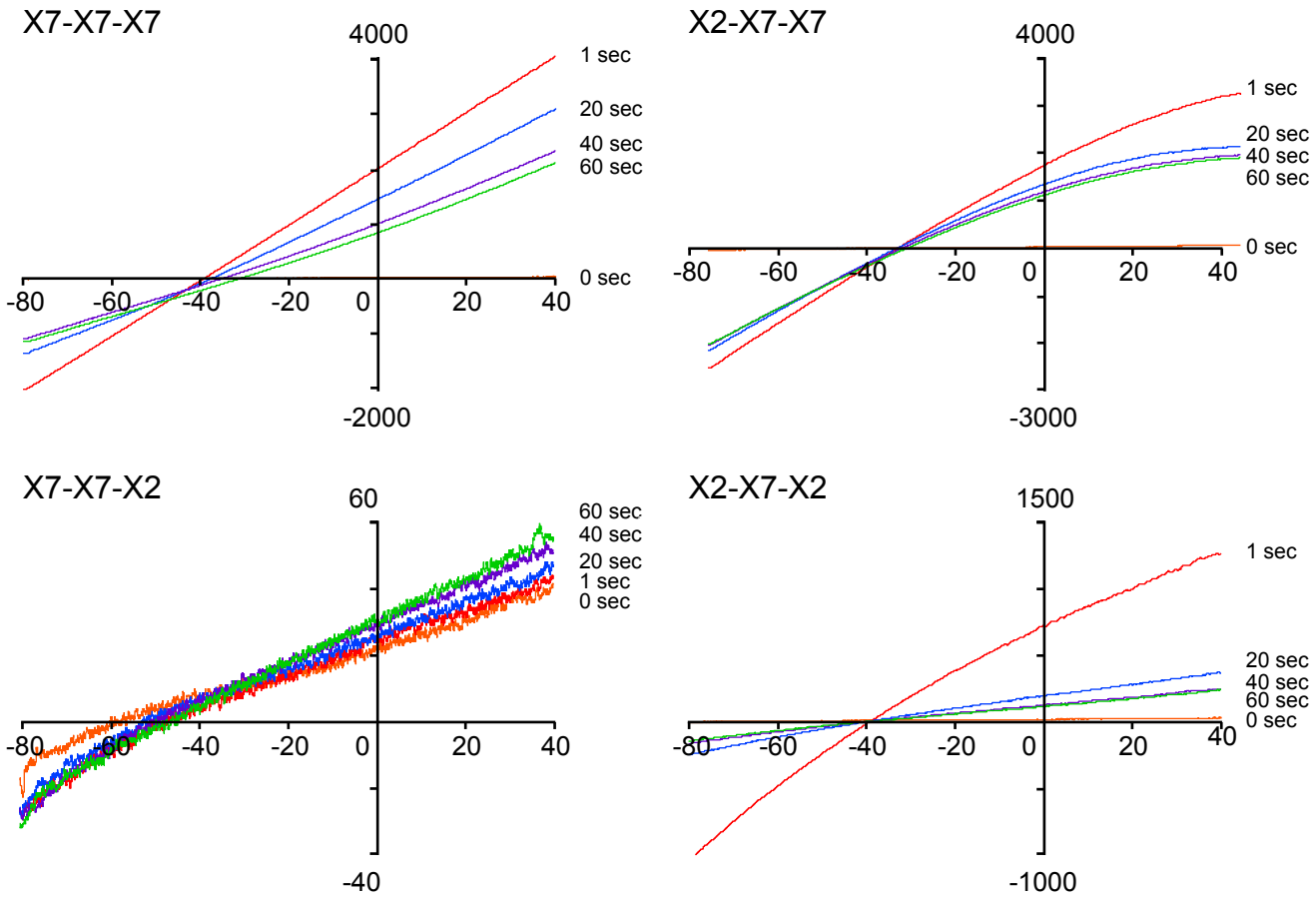
X7-X7-X7
4000
1 sec
20 sec
40 sec
60 sec
0 sec
-80
-60
-40
-20
0
20
40
-2000
X2-X7-X7
4000
1 sec
20 sec
40 sec
60 sec
0 sec
-80
-60
-40
-20
0
20
40
-3000
X7-X7-X2
60
60 sec
40 sec
20 sec
1 sec
0 sec
-80
-60
-40
-20
0
20
40
-40
X2-X7-X2
1500
1 sec
20 sec
40 sec
60 sec
0 sec
-80
-60
-40
-20
0
20
40
-1000

Figure 8

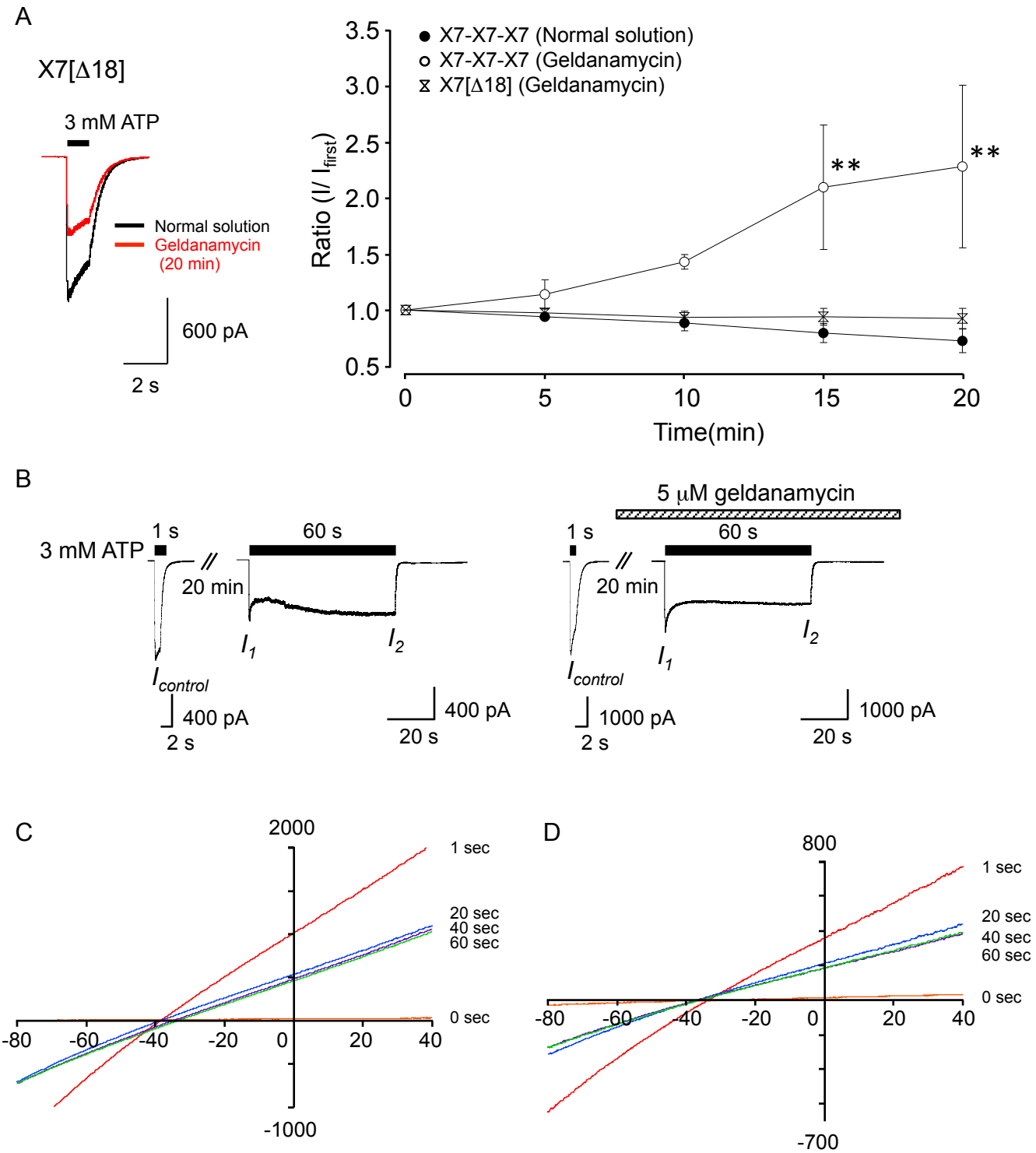
A
X7[Δ18]
3 mM ATP
Normal solution
Geldanamycin
(20 min)
600 pA
2 s
X7-X7-X7 (Normal solution)
X7-X7-X7 (Geldanamycin)
X7[Δ18] (Geldanamycin)
Ratio (I/ I first)
Time(min)
**
**
B
3 mM ATP
1 s
60 s
20 min
I1
I2
Icontrol
400 pA
2 s
400 pA
20 s
5 μM geldanamycin
1000 pA
1000 pA
C
D
1 sec
20 sec
40 sec
60 sec
0 sec
2000
-1000
800
-700

Figure 9

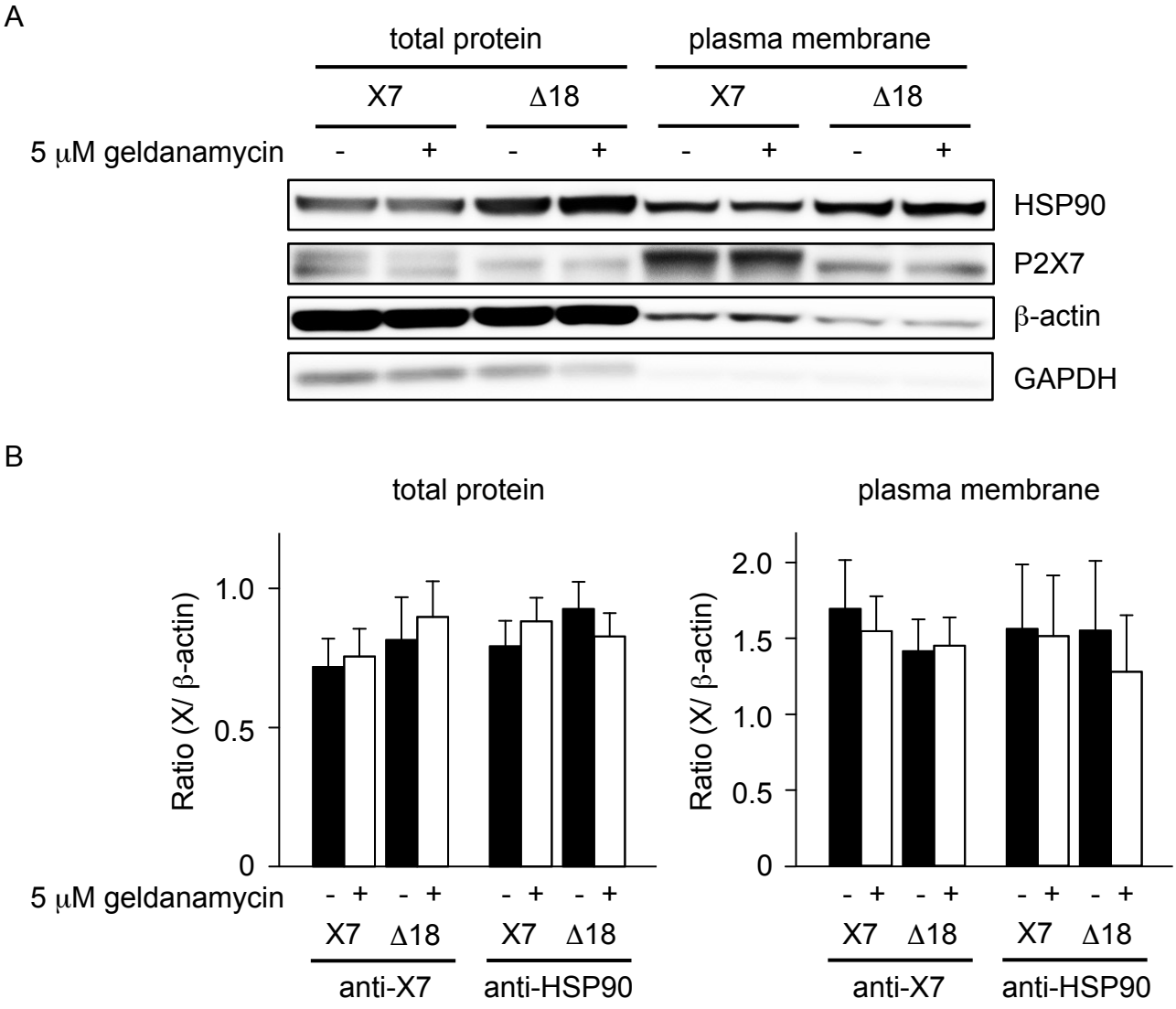
A
total protein
plasma membrane
X7
Δ18
X7
Δ18
5 μM geldanamycin
- + - + - + - +
HSP90
P2X7
β-actin
GAPDH
B
total protein
plasma membrane
Ratio (X/ β-actin)
1.0
0.5
0
2.0
1.5
1.0
0.5
0
5 μM geldanamycin
- + - + - + - +
X7 Δ18 X7 Δ18
anti-X7
anti-HSP90